Letter

Protection of correlation-induced phase instabilities by exceptional susceptibilities

M. Reitner [1], L. Crippa [2], D. R. Fus [1], J. C. Budich [3,4], A. Toschi [1], and G. Sangiovanni [2,*]

[1] *Institute of Solid State Physics, TU Wien, 1040 Vienna, Austria*

[2] *Institut für Theoretische Physik und Astrophysik and Würzburg-Dresden Cluster of Excellence ct.qmat, Universität Würzburg, 97074 Würzburg, Germany*

[3] *Institute of Theoretical Phyiscs, Technische Universität Dresden and Würzburg-Dresden Cluster of Excellence ct.qmat, 01062 Dresden, Germany*

[4] *Max Planck Institute for the Physics of Complex Systems, Nöthnitzer Str. 38, 01187 Dresden, Germany*

(Received 1 July 2023; revised 22 January 2024; accepted 4 April 2024; published 6 May 2024)

At thermal equilibrium, we find that generalized susceptibilities encoding the static physical response properties of Hermitian many-electron systems possess inherent non-Hermitian (NH) matrix symmetries. This leads to the generic occurrence of exceptional points (EPs), i.e., NH spectral degeneracies, in the generalized susceptibilities of prototypical Fermi-Hubbard models, as a function of a single parameter such as chemical potential. We demonstrate that these EPs are necessary to promote correlation-induced thermodynamic instabilities, such as phase separation occurring in the proximity of a Mott transition, to a topologically stable phenomenon.

DOI: 10.1103/PhysRevResearch.6.L022031

Introduction. Topology has been introduced in physics to understand robustness. A pioneering achievement of this approach is the understanding of the quantum Hall effect [1], where the striking quantization of a transverse conductance has been explained in terms of topological properties of Bloch bands [2–4]. Since then, topology has conquered a wide range of physical settings far beyond the band theory of solids [5–15]. As an intriguing direction within this paradigm, here we explain the robustness of phase instabilities in Fermi-Hubbard models by revealing and studying unique topological properties of their generalized susceptibilities [16,17]. These quantities, which encode information on the electronic fluctuations of a many-body system, can be linked to basic observables such as the uniform charge response (isothermal compressibility) $\chi_{\boldsymbol{q}=0}$ [16,18].

Importantly, even for closed many-body systems described by a Hermitian Hamiltonian, such generalized susceptibilities naturally acquire a complex spectrum as matrices in Matsubara frequency space, and are thus subject to a non-Hermitian (NH) topological classification approach [15,19]. There, we identify the emergence of inherent NH symmetries [20,21], requiring merely the physical assumptions of thermal equilibrium and Fermi statistics of the constituents. Under these ubiquitous circumstances, pairs of exceptional points (EPs), i.e., NH spectral degeneracies at which the generalized charge susceptibility matrix $\chi_c^{\nu\nu'}$ becomes nondiagonalizable [22–29], generically occur as a function of a single tuning parameter such as chemical potential (or filling fraction). These EPs are topologically protected by the aforementioned inherent NH symmetry and their splitting in parameter space [see Fig. 1(b) for an illustration].

As a consequence, purely real eigenvalues λ_I of $\chi_c^{\nu\nu'}$ occur in an extended parameter range in between the EPs and generically trigger divergences in the uniform charge response $\chi_{\boldsymbol{q}=0}$ [30] that are robust against small parameter changes [cf. Fig. 1(a) for an illustration]. These divergences in $\chi_{\boldsymbol{q}=0}$ signal the propensity of the correlated system to undergo a thermodynamic phase separation between a compressible metallic and an almost incompressible "bad metal" phase, often occurring in the proximity of Mott metal-to-insulator transitions [30–34]. This phase separation can be viewed, in many respects, as the electronic counterpart of the liquid gas transition for water molecules.

Non-Hermitian topology and EPs have been widely discussed in systems where the Bloch band structure has been augmented by dissipative terms of various physical origin, ranging from scattering rates of quasiparticles [35–45] to gain and loss in optical systems [46–52]. There, the experimental visibility of NH signatures is oftentimes limited by the overall blurring introduced by imaginary damping terms in the dissipative time evolution. By contrast, since the generalized susceptibilities at the heart of our present analysis do not relate to effective complex energy spectra, their NH topology has a direct impact on natural observables, independent of idealistic assumptions on temperature and without the need for complex multiorbital models, respectively.

NH symmetries of generalized susceptibilities. The central objects of our analysis are four-point functions describing the propagation of a particle-hole pair [see Fig. 2(b)] in the setting of a time-independent Hamiltonian H at thermal equilibrium. These are expressed as matrices of two fermionic Matsubara frequencies ν and ν', where $\nu^{(\prime)} = (2n^{(\prime)} + 1)\pi/\beta$, $n^{(\prime)} \in \mathbb{Z}$, and $\beta = 1/T$ is the inverse temperature. In the literature, such quantities are referred to as generalized susceptibilities, since

* giorgio.sangiovanni@uni-wuerzburg.de

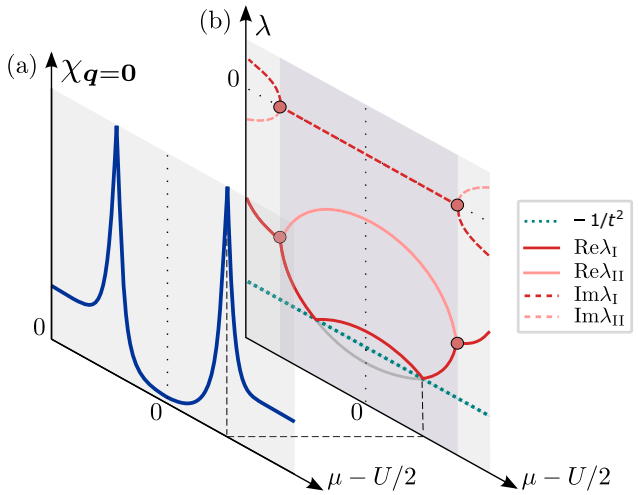

FIG. 1. Schematic illustration of the enhancement of the uniform charge response $\chi_{\boldsymbol{q}=\boldsymbol{0}}$ (a) triggered by the eigenvalue λ_I reaching the condition $\lambda_\mathrm{I} = -1/t^2$ (b). The chemical potential μ at which the divergence happens is located within a finite range, bounded by the EPs [red dots on (b)]. If a divergence is found, no small perturbation can wash it out, as the intersection between the "rectified" λ_I curve (thin gray line) and the $-1/t^2$ limit can only be continuously shifted.

they yield static physical response functions when summed over both fermionic frequencies [53]. Specifically, we define them as

$$\chi^{\nu\nu'}_{\mathrm{ph},\alpha_1\ldots\alpha_4} = \overbrace{\langle \mathcal{T} c^\dagger_{\nu\alpha_1} c_{\nu\alpha_2} c^\dagger_{\nu'\alpha_3} c_{\nu'\alpha_4}\rangle}^{G^{(2)\nu\nu'}_{\alpha_1\ldots\alpha_4}} - \langle \mathcal{T} c^\dagger_{\nu\alpha_1} c_{\nu\alpha_2}\rangle\langle \mathcal{T} c^\dagger_{\nu'\alpha_3} c_{\nu'\alpha_4}\rangle \tag{1}$$

[illustrated in Fig. 2(a)], where $\mathcal{T}$ denotes the imaginary time ordering operator, $\langle \ldots \rangle = 1/Z\,\mathrm{Tr}(\mathrm{e}^{-\beta H}\ldots)$ the thermal expectation value, $c^{(\dagger)}_{\nu\alpha_i} = \frac{1}{\sqrt{\beta}}\int_0^\beta \mathrm{d}\tau \mathrm{e}^{(-)\mathrm{i}\nu\tau}\mathrm{e}^{H\tau} c^{(\dagger)}_{\alpha_i}\mathrm{e}^{-H\tau}$ the Fourier transform of the (creation) annihilation operators [54], and $G^{(2)\nu\nu'}_{\alpha_1\ldots\alpha_4}$ the two-particle Green's function. α_i refers to, in principle, any of the degrees of freedom of the model (momenta, spin, orbital, etc.). Some properties of $\chi^{\nu\nu'}_{\mathrm{ph},\alpha_1\ldots\alpha_4}$ have been already analyzed in Refs. [16,17,53,55,56]. In this work, we are investigating the topological properties of the corresponding eigenvalue spectrum.

Taking the complex conjugate of Eq. (1) and considering $(c^\dagger_\nu)^* = -c_{-\nu}$, and $(c_\nu)^* = -c^\dagger_{-\nu}$ inside of $\langle \ldots \rangle$, one obtains $(\chi^{\nu\nu'}_{\mathrm{ph},\alpha_1\ldots\alpha_4})^* = \chi^{-\nu'-\nu}_{\mathrm{ph},\alpha_4\ldots\alpha_1}$ [57]. With simple further manipulations on the indices leaving $\langle \mathcal{T}\ldots\rangle$ invariant, this leads to $(\chi^{\nu\nu'}_{\mathrm{ph},\alpha_1\alpha_2\alpha_3\alpha_4})^* = \chi^{-\nu-\nu'}_{\mathrm{ph},\alpha_2\alpha_1\alpha_4\alpha_3}$. The latter mathematical object has the form of a matrix with coefficients $\chi^{\beta\beta'}_{\mathrm{ph}}$, which, crucially, satisfies the relation

$$\chi^{\beta\beta'}_{\mathrm{ph}} = \sum_{\beta_1\beta_2} \Pi^{\beta\beta_1}\left(\chi^{\beta_1\beta_2}_{\mathrm{ph}}\right)^* \Pi^{\beta_2\beta'}, \tag{2}$$

where $\Pi^{\beta\beta'}$ is the permutation matrix $\beta := (\nu, \alpha_1, \alpha_2) \to \beta' := (-\nu, \alpha_2, \alpha_1)$. This property has important consequences for the eigenvalues λ of χ_{ph}, which belongs to the class of κ-real matrices $\boldsymbol{K}_r = \boldsymbol{\Pi}\boldsymbol{K}^*_r\boldsymbol{\Pi}$ [58], where $\boldsymbol{\Pi}$ refers to any permutation matrix. These have been shown [58] to have a

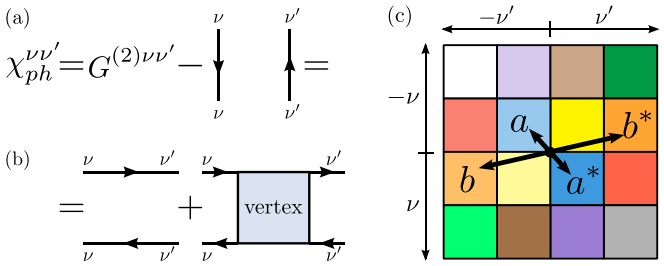

FIG. 2. Panels (a) and (b) are a diagrammatic representation of the generalized susceptibility, as given in Eq. (1), using $\langle \mathcal{T} c_\nu c^\dagger_{\nu'}\rangle = \nu \longrightarrow \nu' = \delta^{\nu\nu'} G(\mathrm{i}\nu)$ and $\langle \mathcal{T} c_\nu c^\dagger_{\nu'}\rangle = \nu \longleftarrow \nu' = -\delta^{\nu\nu'} G(\mathrm{i}\nu)$, where $G(\mathrm{i}\nu)$ refers to the one-particle Green's function (here, we dropped the α_i indices for clarity). Panel (c), schematic illustration of the centro-Hermitian matrix symmetry.

characteristic polynomial with real coefficients and, hence, either real or complex conjugate eigenvalues due to the fundamental theorem of algebra. A relevant subclass of κ-real matrices are centro-Hermitian matrices [59,60], which are invariant under a transformation that combines complex conjugation with centrosymmetry, as illustrated in Fig. 2(c).

In the following, we consider the local generalized charge susceptibility $\chi_c^{\nu\nu'} = \frac{1}{2}\sum_{\sigma\sigma'}\chi^{\nu\nu'}_{\mathrm{ph},\sigma\sigma\sigma'\sigma'}$ of a one-orbital model that satisfies the following relation:

$$\left(\chi_c^{\nu\nu'}\right)^* = \frac{1}{2}\sum_{\sigma\sigma'}\chi^{-\nu-\nu'}_{\mathrm{ph},\sigma\sigma\sigma'\sigma'} = \chi_c^{-\nu-\nu'} \tag{3}$$

and is therefore a centro-Hermitian matrix. In addition, if the Hamiltonian possesses specific symmetries, these can impose even stricter matrix properties. For instance, for particle-hole symmetry (PHS) $\chi_c^{\nu\nu'}$ becomes real and has only real eigenvalues [17,56].

Minimal model for exceptional susceptibilities. To illustrate our general findings, we consider a 2×2 matrix $\chi^{2\times2}_{\mathrm{ph}}$ obeying the centro-Hermitian condition:

$$\chi^{2\times2}_{\mathrm{ph}} = \begin{pmatrix} a+\mathrm{i}b & c-\mathrm{i}d \\ c+\mathrm{i}d & a-\mathrm{i}b \end{pmatrix} = a\cdot\mathbb{I} + \vec{v}\cdot\vec{\sigma}, \tag{4}$$

where $a, b, c, d \in \mathbb{R}$, and $\vec{v} = \vec{v}_R + i\vec{v}_I = (c, d, 0) + i(0, 0, b)$ is a complex vector. The a parameter can be safely disregarded, as it only amounts to a rigid eigenvalue shift. EPs are globally stable for a two- or higher-dimensional parameter space, because for the matrix to become nondiagonalizable, two conditions $(v_R^2 - v_I^2 = 0,\ \vec{v}_R\cdot\vec{v}_I = 0)$ have to be simultaneously satisfied. It is immediate to see that the centro-Hermitian property implies that the second is always fulfilled. It is then sufficient, for the exceptional points to manifest, that $c^2 + d^2 - b^2 = 0$, which implies that even in a one-dimensional space, EPs—if any are present—will be globally robust against any perturbation representable by a matrix of the form given in Eq. (4) [61]. Crucially, no other perturbation can arise, because the centro-Hermitian condition does not originate from any further symmetry, but it is an intrinsic consequence of the time independence of H and a defined quantum (here: Fermi-Dirac) statistics [62]. The occurrence of these stable EPs generically mark the borders of regions with complex conjugate pairs on the one

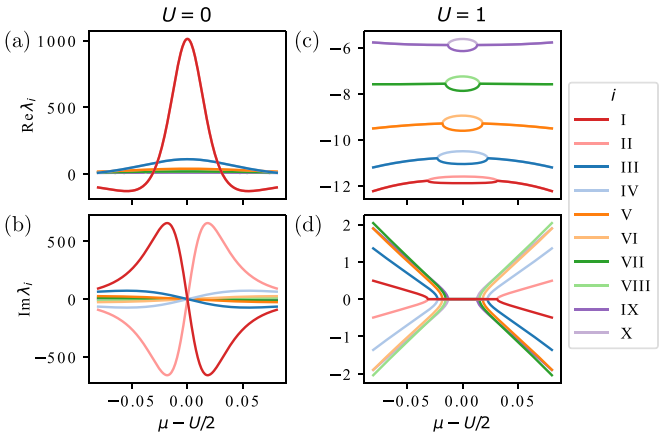

FIG. 3. Real part (top row) and imaginary part (bottom row) of the eigenvalues λ_i of $\chi_c^{\nu\nu'}$ for the atomic limit (AL) at temperature $T = 1/100$, $U = 0$ (a), (b) and at $U = 1$ (c), (d) as functions of chemical potential away from particle-hole symmetry (PHS) at $\mu = U/2$. The ten eigenvalues which are lowest in $\mathrm{Re}\,\lambda_i$ at $U = 1$ are displayed.

hand and real and distinct eigenvalues on the other hand. On the contrary, if we additionally impose PHS, $\chi_{\mathrm{ph}}^{2\times2}$ becomes purely real and symmetric ($b, d = 0$), which implies that the only solution of the two conditions for the EPs will be for $\vec{v}_R = \vec{v}_I = 0$. This is known in literature as a diabolic point, which is effectively concurrent with a Hermitian degeneracy [15] and, indeed, generally requires fine tuning.

Analytical study of the atomic limit. As the simplest physical platform to exemplify the spectral properties of $\chi_c^{\nu\nu'}$, we now study the exactly solvable atomic limit of the Hubbard model (AL)

$$H = -\mu(n_\uparrow + n_\downarrow) + U n_\uparrow n_\downarrow, \tag{5}$$

where μ is the chemical potential, $n_\sigma = c_\sigma^\dagger c_\sigma$ the occupation of an electron with spin σ, and U the on-site Coulomb repulsion given in arbitrary units of energy. This model fulfills PHS if $\mu = U/2$ and is in general SU(2) symmetric [63]. In the case of zero interaction $U = 0$, the local generalized charge susceptibility reads

$$\chi_c^{\nu\nu'} \overset{U=0}{=} -G(\mathrm{i}\nu)G(\mathrm{i}\nu')\delta^{\nu\nu'} = -\frac{\delta^{\nu\nu'}}{(\mathrm{i}\nu + \mu)^2}, \tag{6}$$

where $G(\mathrm{i}\nu) = \langle \mathcal{T} c_{\nu\sigma}^\dagger c_{\nu\sigma} \rangle$ is the one-particle Green's function. $\chi_c^{\nu\nu'}$ is diagonal, hence the eigenvalues can be immediately read from Eq. (6). These become doubly degenerate ($\lambda_\nu = \lambda_{-\nu} = 1/\nu^2$) at PHS, i.e., $\mu = 0$, while they form complex conjugate pairs ($\lambda_\nu = \lambda_{-\nu}^*$) at finite μ. In the left column of Fig. 3 the real (i) and imaginary part (ii) of λ_i are shown for different μ at finite temperature $T = 1/100$.

At finite interaction $U > 0$, $\chi_c^{\nu\nu'}$ becomes a more complicated expression [17,64–66], given in the Supplemental Material [67]. The crucial point is the appearance of progressively larger off-diagonal components. The resulting eigenvalues λ_i are shown in the right column of Fig. 3. Significantly, at PHS, λ_i are still purely real but no longer degenerate. Importantly, this remains true in a finite region of μ around $U/2$. Far away from PHS, however, the effect of the interaction weakens, and all eigenvalues become complex conjugate pairs. To switch between these two regimes, two eigenvalues have to coalesce: this creates a pair of distinct EPs in μ space, which delimit and protect the real-eigenvalue "lens"-shaped structure [Fig. 3(c)]. In the 2×2 picture of Eq. (4), we can identify the interaction U as responsible for the presence of the off-diagonal finite elements c and d in the matrix, and the finite μ for the diagonal element b, which are the two ingredients necessary to satisfy the EP conditions. Hence, for the AL, any finite value of U will result in exceptional points away from PHS and a finite-size real eigenvalue lens shape.

Implications on correlation-induced instabilities. We now turn to a more generic scenario, namely the single-orbital Hubbard Hamiltonian on a lattice:

$$H = -t \sum_{\langle ij\rangle,\sigma} (c_{i\sigma}^\dagger c_{j\sigma} + c_{j\sigma}^\dagger c_{i\sigma}) - \mu \sum_{i,\sigma} n_{i\sigma} + U \sum_i n_{i\uparrow} n_{i\downarrow} \tag{7}$$

with constant hopping t between neighboring sites i and j. This model is again SU(2) symmetric and for $\mu = U/2$ it fulfills PHS. Except for one or infinite spatial dimensions, the model has not been solved analytically. In order to get a nonperturbative, albeit approximated many-body solution, we use dynamical mean-field theory (DMFT) (which becomes exact only in the limit of infinite dimensions) [68,69] with a continuous-time quantum Monte Carlo solver from *w2dynamics* [70]. As shown in Ref. [30], the eigenvalues λ_i and the corresponding eigenvectors v_i^ν of the local generalized susceptibility $\chi_c^{\nu\nu'}$ ($\sum_{\nu'} \chi_c^{\nu\nu'} v_i^{\nu'} = \lambda_i v_i^\nu$) play an important role for the response functions of the whole lattice: they lead to an enhancement and, in some cases, to a divergence of the uniform (i.e., for zero transfer momentum $\mathbf{q} = 0$) susceptibility. In particular, for the Bethe lattice with infinite connectivity (where DMFT is exact), the static uniform charge response, obtained by summing the generalized susceptibility over all Matsubara frequencies $\chi_{\mathbf{q}=0} = \sum_{\nu\nu'} \chi_{\mathbf{q}=0}^{\nu\nu'}$, can be re-expressed in terms of λ_i and corresponding weights $w_i = (\sum_\nu (v_i^{-1})^\nu)(\sum_{\nu'} v_i^{\nu'})$. This leads to the following expression

$$\chi_{\mathbf{q}=0} = \frac{1}{\beta} \sum_i \left(\frac{1}{\lambda_i} + t^2 \right)^{-1} w_i, \tag{8}$$

which diverges—thus inducing a phase instability in the charge sector—when one eigenvalue fulfills the condition $\lambda_i = -1/t^2$. Close to this condition, λ_i gives the dominating contribution to the charge response and determines the stability of the physical solution [71]. Importantly, this is possible only when λ_i is real [72].

Although Eq. (8) is only exact in the case of the Bethe lattice, numerical calculations have shown [30] that it holds also for a square lattice if t is replaced by a temperature- and μ-dependent $t_{\mathrm{eff}}(\mu, T)$. Here, the central role of EPs becomes apparent: their presence guarantees that the imaginary part of λ_i remains zero in the whole extended region of the lens shape. In other words, the possibility of inducing a divergence in $\chi_{\mathbf{q}=0}$ is not accidental and does not rely on a fine tuning of U, T, and μ: the phase instability is in fact topologically protected. For the square lattice, this is illustrated in Fig. 4, where we plot the real (a) and imaginary part (b) of the eigenvalues λ_i of the local charge susceptibility $\chi_c^{\nu\nu'}$ close to the critical

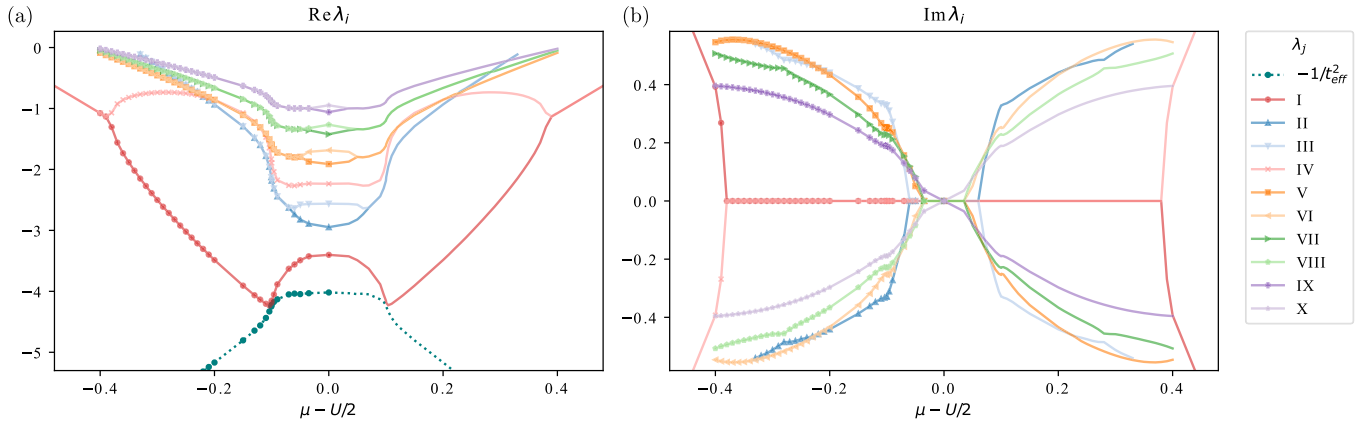

FIG. 4. Real part (a) and imaginary part (b) of the eigenvalues λ_i of $\chi_c^{\nu\nu'}$ for the square lattice Hubbard model (with half bandwidth $D = 4t = 1$) solved within DMFT as a function of chemical potential away from PHS at $\mu = U/2$. Interaction strength $U = 2.4$ and temperature $T = 1/53$ coincide with Ref. [30] to show the situation close to the thermodynamic instability. Calculated data are displayed as dots, the positive $(\mu - U/2)$ axis is mapped from the negative one, exploiting the symmetry of the model considered. The ten eigenvalues which are lowest in Re λ_i at $\mu - U/2 = 0$ are displayed.

point of the phase separation (cf. sketch in Fig. 1). Here, the lowest eigenvalue λ_I satisfies (up to numerical accuracy) the condition $\lambda_I = -1/t_{\text{eff}}^2$ in the region of the lens shape. Hence, the phase instability condition is also fulfilled for any further reduction of the temperature T (or for any moderate reduction of the interaction U). In particular, at lower T, we enter a regime, where a first order phase separation occurs. This regime is, thus, characterized by two locally stable DMFT solutions (i.e., two coexisting values of λ_I), corresponding to a less correlated metallic and a "bad metal" phase (connected by an instable solution, where $\lambda_I < -1/t_{\text{eff}}^2$ [71]). Here, the topological robust arguments related to the condition $\lambda_I = -1/t_{\text{eff}}^2$ remain nonetheless applicable, albeit to the two corresponding metastable solutions [73].

Finally, let us notice that a negative eigenvalue is a necessary condition for the instability criterion to be fulfilled [30]. Remarkably, the role of the negative eigenvalues in the generalized charge susceptibility has been recently related to the local moment formation [74–77] and, on a more formal level, to divergences of the irreducible vertex function and the multivaluedness of the Luttinger-Ward functional [17,30,34,56,74–98]. Therefore, these negative eigenvalues can be regarded as a feature of strong electronic correlations, which cannot be commonly described by "perturbative" theories, e.g., the random phase approximation. However, the considerations behind Eq. (8) are not solely restricted to negative eigenvalues. They can be also applied to the opposite case, where a positive eigenvalue reaching a maximum (e.g., $\lambda_i = 1/t_{\text{eff}}^2$) triggers a phase instability, such as the antiferromagnetic transitions of the Hubbard model [99]. Thus, in these strongly correlated systems, the presence of EPs is found to generally promote phase instabilities in the ph channel [100] to a stable phenomenon, and thereby enables the instabilities to naturally occur for a finite range in parameter space.

Conclusion. We have found the opening of an EP phase for the associated eigenvalues of the static local susceptibility in the U/μ phase diagram of models for correlated electron systems. The remarkable consequence is that the interaction-induced charge instabilities, such as the phase separation occurring close to the Mott metal-to-insulator transition in the Hubbard model, do not need any fine tuning but can occur in an entire finite range of parameters. This unexpected global robustness is a consequence of the peculiar centro-Hermitian form of the susceptibility matrix, which is not dictated by some *ad hoc* antiunitary symmetry but by the time independence of H and the intrinsic nature of Fermi-Dirac statistics.

The susceptibility EPs represent a clear-cut and compelling manifestation of non-Hermitian topology, surpassing the conventional realizations based on spectral functions. This phenomenon is indeed ubiquitous even in the simplest correlated fermion models and does not require any assumption on the interaction, nor any specific choice of non-Hermitian Hamiltonian terms. Our results call for future investigations beyond the local correlation effects on the charge sector considered here, e.g., of the spin or particle-particle channel and including nonlocal correlations in the description. Further, one could also search for higher order exceptional degeneracies in the susceptibility spectrum and explore the respective consequences on the phase instabilities. This may open new doors to experimentally detectable hallmarks of non-Hermitian topology.

Acknowledgments. We thank P. Chalupa-Gantner, H. Eßl, and P. Oberleitner for insightful discussions, and S. Di Cataldo, P. Kappl, and P. Worm for helpful comments. M.R. acknowledges support as a recipient of a DOC fellowship of the Austrian Academy of Sciences and financial support from the Austrian Science Fund (FWF), within Project I 5487. A.T. acknowledges the Austrian Science Fund (FWF) for Project I 5868 (part of the FOR 5249 [QUAST] of the German Science Foundation, DFG). L.C., J.C.B., and G.S. acknowledge financial support by the Deutsche Forschungsgemeinschaft (DFG, German Research Foundation) under Germany's Excellence Strategy EXC2147 "ct.qmat" (Project ID 390858490), as well as through Project-ID 258499086 SFB 1170 "ToCoTronics" and Project-ID 247310070 - SFB 1143. Calculations have been performed on the Vienna Scientific Cluster (VSC).

[1] K. v. Klitzing, G. Dorda, and M. Pepper, New method for high-accuracy determination of the fine-structure constant based on quantized Hall resistance, Phys. Rev. Lett. **45**, 494 (1980).

[2] R. B. Laughlin, Quantized Hall conductivity in two dimensions, Phys. Rev. B **23**, 5632(R) (1981).

[3] B. I. Halperin, Quantized Hall conductance, current-carrying edge states, and the existence of extended states in a two-dimensional disordered potential, Phys. Rev. B **25**, 2185 (1982).

[4] D. J. Thouless, M. Kohmoto, M. P. Nightingale, and M. den Nijs, Quantized Hall conductance in a two-dimensional periodic potential, Phys. Rev. Lett. **49**, 405 (1982).

[5] B. Bernevig and T. Hughes, *Topological Insulators and Topological Superconductors* (Princeton University Press, Princeton, 2013).

[6] M. Z. Hasan and C. L. Kane, *Colloquium:* Topological insulators, Rev. Mod. Phys. **82**, 3045 (2010).

[7] X.-L. Qi and S.-C. Zhang, Topological insulators and superconductors, Rev. Mod. Phys. **83**, 1057 (2011).

[8] X. Chen, Z.-C. Gu, and X.-G. Wen, Local unitary transformation, long-range quantum entanglement, wave function renormalization, and topological order, Phys. Rev. B **82**, 155138 (2010).

[9] S. D. Huber, Topological mechanics, Nat. Phys. **12**, 621 (2016).

[10] B. Bradlyn, L. Elcoro, J. Cano, M. G. Vergniory, Z. Wang, C. Felser, M. I. Aroyo, and B. A. Bernevig, Topological quantum chemistry, Nature (London) **547**, 298 (2017).

[11] T. Ozawa, H. M. Price, A. Amo, N. Goldman, M. Hafezi, L. Lu, M. C. Rechtsman, D. Schuster, J. Simon, O. Zilberberg, and I. Carusotto, Topological photonics, Rev. Mod. Phys. **91**, 015006 (2019).

[12] Z. Gong, Y. Ashida, K. Kawabata, K. Takasan, S. Higashikawa, and M. Ueda, Topological phases of non-Hermitian systems, Phys. Rev. X **8**, 031079 (2018).

[13] Z.-D. Song, L. Elcoro, and B. A. Bernevig, Twisted bulk-boundary correspondence of fragile topology, Science **367**, 794 (2020).

[14] H. Xue, Y. Yang, and B. Zhang, Topological acoustics, Nat. Rev. Mater. **7**, 974 (2022).

[15] E. J. Bergholtz, J. C. Budich, and F. K. Kunst, Exceptional topology of non-Hermitian systems, Rev. Mod. Phys. **93**, 015005 (2021).

[16] G. Rohringer, A. Valli, and A. Toschi, Local electronic correlation at the two-particle level, Phys. Rev. B **86**, 125114 (2012).

[17] P. Thunström, O. Gunnarsson, S. Ciuchi, and G. Rohringer, Analytical investigation of singularities in two-particle irreducible vertex functions of the Hubbard atom, Phys. Rev. B **98**, 235107 (2018).

[18] N. Bickers, Self-consistent many-body theory for condensed matter systems, in *Theoretical Methods for Strongly Correlated Electrons* (Springer, New York, 2004), pp. 237–296.

[19] K. Kawabata, K. Shiozaki, M. Ueda, and M. Sato, Symmetry and topology in non-Hermitian physics, Phys. Rev. X **9**, 041015 (2019).

[20] D. Bernard and A. LeClair, A classification of 2D random Dirac fermions, J. Phys. A: Math. Gen. **35**, 2555 (2002).

[21] C.-H. Liu and S. Chen, Topological classification of defects in non-Hermitian systems, Phys. Rev. B **100**, 144106 (2019).

[22] M. V. Berry, Physics of nonhermitian degeneracies, Czech. J. Phys. **54**, 1039 (2004).

[23] W. D. Heiss and H. L. Harney, The chirality of exceptional points, Eur. Phys. J. D **17**, 149 (2001).

[24] W. D. Heiss, The physics of exceptional points, J. Phys. A: Math. Theor. **45**, 444016 (2012).

[25] D. Heiss, Circling exceptional points, Nat. Phys. **12**, 823 (2016).

[26] H. Shen, B. Zhen, and L. Fu, Topological band theory for non-Hermitian Hamiltonians, Phys. Rev. Lett. **120**, 146402 (2018).

[27] K. Kawabata, T. Bessho, and M. Sato, Classification of exceptional points and non-Hermitian topological semimetals, Phys. Rev. Lett. **123**, 066405 (2019).

[28] Z. Yang, A. P. Schnyder, J. Hu, and C.-K. Chiu, Fermion doubling theorems in two-dimensional non-Hermitian systems for Fermi points and exceptional points, Phys. Rev. Lett. **126**, 086401 (2021).

[29] M. Stålhammar and E. J. Bergholtz, Classification of exceptional nodal topologies protected by $\mathcal{PT}$ symmetry, Phys. Rev. B **104**, L201104 (2021).

[30] M. Reitner, P. Chalupa, L. Del Re, D. Springer, S. Ciuchi, G. Sangiovanni, and A. Toschi, Attractive effect of a strong electronic repulsion: The physics of vertex divergences, Phys. Rev. Lett. **125**, 196403 (2020).

[31] G. Kotliar, S. Murthy, and M. J. Rozenberg, Compressibility divergence and the finite temperature Mott transition, Phys. Rev. Lett. **89**, 046401 (2002).

[32] P. Werner and A. J. Millis, Doping-driven Mott transition in the one-band Hubbard model, Phys. Rev. B **75**, 085108 (2007).

[33] M. Eckstein, M. Kollar, M. Potthoff, and D. Vollhardt, Phase separation in the particle-hole asymmetric Hubbard model, Phys. Rev. B **75**, 125103 (2007).

[34] R. Nourafkan, M. Côté, and A.-M. S. Tremblay, Charge fluctuations in lightly hole-doped cuprates: Effect of vertex corrections, Phys. Rev. B **99**, 035161 (2019).

[35] T. Yoshida, R. Peters, and N. Kawakami, Non-Hermitian perspective of the band structure in heavy-fermion systems, Phys. Rev. B **98**, 035141 (2018).

[36] K. Kimura, T. Yoshida, and N. Kawakami, Chiral-symmetry protected exceptional torus in correlated nodal-line semimetals, Phys. Rev. B **100**, 115124 (2019).

[37] R. Aquino and D. G. Barci, Two-dimensional Fermi liquid dynamics with density-density and quadrupolar interactions, Phys. Rev. B **100**, 115117 (2019).

[38] T. Yoshida, R. Peters, N. Kawakami, and Y. Hatsugai, Exceptional band touching for strongly correlated systems in equilibrium, Prog. Theor. Exp. Phys. **2020**, 12A109 (2020).

[39] R. Aquino and D. G. Barci, Exceptional points in Fermi liquids with quadrupolar interactions, Phys. Rev. B **102**, 201110 (2020).

[40] Y. Nagai, Y. Qi, H. Isobe, V. Kozii, and L. Fu, DMFT reveals the non-Hermitian topology and Fermi arcs in heavy-fermion systems, Phys. Rev. Lett. **125**, 227204 (2020).

[41] R. Rausch, R. Peters, and T. Yoshida, Exceptional points in the one-dimensional Hubbard model, New J. Phys. **23**, 013011 (2021).

[42] C. Lehmann, M. Schüler, and J. C. Budich, Dynamically induced exceptional phases in quenched interacting semimetals, Phys. Rev. Lett. **127**, 106601 (2021).

[43] L. Crippa, G. Sangiovanni, and J. C. Budich, Spontaneous formation of exceptional points at the onset of magnetism, Phys. Rev. Lett. **130**, 186403 (2023).

[44] B. Michen, T. Micallo, and J. C. Budich, Exceptional non-Hermitian phases in disordered quantum wires, Phys. Rev. B **104**, 035413 (2021).

[45] B. Michen and J. C. Budich, Mesoscopic transport signatures of disorder-induced non-Hermitian phases, Phys. Rev. Res. **4**, 023248 (2022).

[46] M.-A. Miri and A. Alù, Exceptional points in optics and photonics, Science **363**, eaar7709 (2019).

[47] S. Weimann, M. Kremer, Y. Plotnik, Y. Lumer, S. Nolte, K. G. Makris, M. Segev, M. C. Rechtsman, and A. Szameit, Topologically protected bound states in photonic parity–time-symmetric crystals, Nat. Mater. **16**, 433 (2017).

[48] K. Takata and M. Notomi, Photonic topological insulating phase induced solely by gain and loss, Phys. Rev. Lett. **121**, 213902 (2018).

[49] Y. Zhiyenbayev, Y. Kominis, C. Valagiannopoulos, V. Kovanis, and A. Bountis, Enhanced stability, bistability, and exceptional points in saturable active photonic couplers, Phys. Rev. A **100**, 043834 (2019).

[50] Y. Ashida, Z. Gong, and M. Ueda, Non-Hermitian physics, Adv. Phys. **69**, 249 (2020).

[51] S. Weidemann, M. Kremer, T. Helbig, T. Hofmann, A. Stegmaier, M. Greiter, R. Thomale, and A. Szameit, Topological funneling of light, Science **368**, 311 (2020).

[52] H. Menke and M. M. Hirschmann, Topological quantum wires with balanced gain and loss, Phys. Rev. B **95**, 174506 (2017).

[53] G. Rohringer, H. Hafermann, A. Toschi, A. A. Katanin, A. E. Antipov, M. I. Katsnelson, A. I. Lichtenstein, A. N. Rubtsov, and K. Held, Diagrammatic routes to nonlocal correlations beyond dynamical mean field theory, Rev. Mod. Phys. **90**, 025003 (2018).

[54] Here we have shortened the notation of the Fourier transform of the time-ordered operators to make their properties in the following derivations more transparent, in Eq. 1 the time ordering is acting first on the time arguments of the operators and then the respective integrals are performed.

[55] G. Rohringer, New routes toward a theoretical treatment of nonlocal electronic correlations, Ph.D. thesis, Technischen Universität Wien, 2014.

[56] D. Springer, P. Chalupa, S. Ciuchi, G. Sangiovanni, and A. Toschi, Interplay between local response and vertex divergences in many-fermion systems with on-site attraction, Phys. Rev. B **101**, 155148 (2020).

[57] A detailed derivation can be found in the Supplemental Material [67].

[58] R. D. Hill and S. R. Waters, On κ-real and κ-Hermitian matrices, Linear Algebra Appl. **169**, 17 (1992).

[59] A. Lee, Centrohermitian and skew-centrohermitian matrices, Linear Algebra Appl. **29**, 205 (1980), Special Volume Dedicated to Alson S. Householder.

[60] R. D. Hill, R. G. Bates, and S. R. Waters, On centrohermitian matrices, SIAM J. Matrix Anal. Appl. **11**, 128 (1990).

[61] J. C. Budich, J. Carlström, F. K. Kunst, and E. J. Bergholtz, Symmetry-protected nodal phases in non-Hermitian systems, Phys. Rev. B **99**, 041406 (2019).

[62] See the Supplemental Material for a short discussion on the differences between the susceptibility matrix properties of Fermi-Dirac and Bose-Einstein statistics [67].

[63] For the effect of the SU(2)-symmetry on the generalized susceptibilities, see Refs. [16,18].

[64] S. Pairault, D. Sénéchal, and A.-M. S. Tremblay, Strong-coupling perturbation theory of the Hubbard model, Eur. Phys. J. B **16**, 85 (2000).

[65] D. R. Fus, Breakdown of the many-electron perturbation expansion beyond particle-hole symmetry: An atomic limit study, Bachelor thesis, Technischen Universität Wien, 2022.

[66] H. Eßl, M. Reitner, G. Sangiovanni, and A. Toschi, General shiba mapping for on-site four-point correlation functions, arXiv:2402.16115 [cond-mat.str-el].

[67] See Supplemental Material at http://link.aps.org/supplemental/10.1103/PhysRevResearch.6.L022031 for more details on the symmetry properties of the generalized susceptibilities and further information.

[68] W. Metzner and D. Vollhardt, Correlated lattice fermions in $d = \infty$ dimensions, Phys. Rev. Lett. **62**, 324 (1989).

[69] A. Georges, G. Kotliar, W. Krauth, and M. J. Rozenberg, Dynamical mean-field theory of strongly correlated fermion systems and the limit of infinite dimensions, Rev. Mod. Phys. **68**, 13 (1996).

[70] M. Wallerberger, A. Hausoel, P. Gunacker, A. Kowalski, N. Parragh, F. Goth, K. Held, and G. Sangiovanni, w2dynamics: Local one- and two-particle quantities from dynamical mean field theory, Comput. Phys. Commun. **235**, 388 (2019).

[71] A. Kowalski, M. Reitner, L. D. Re, M. Chatzieleftheriou, A. Amaricci, A. Toschi, L. de' Medici, G. Sangiovanni, and T. Schäfer, Thermodynamic stability at the two-particle level, arXiv:2309.11108 [cond-mat.str-el].

[72] Further, the corresponding weight must be $w_i \neq 0$, which is, in general, fulfilled away from PHS for $\mu \neq U/2$ [30].

[73] A schematic illustration of this regime can be found in the Supplemental Material [67].

[74] P. Chalupa, T. Schäfer, M. Reitner, D. Springer, S. Andergassen, and A. Toschi, Fingerprints of the local moment formation and its Kondo screening in the generalized susceptibilities of many-electron problems, Phys. Rev. Lett. **126**, 056403 (2021).

[75] T. B. Mazitov and A. A. Katanin, Local magnetic moment formation and Kondo screening in the half-filled single-band Hubbard model, Phys. Rev. B **105**, L081111 (2022).

[76] T. B. Mazitov and A. A. Katanin, Effect of local magnetic moments on spectral properties and resistivity near interaction- and doping-induced Mott transitions, Phys. Rev. B **106**, 205148 (2022).

[77] S. Adler, F. Krien, P. Chalupa-Gantner, G. Sangiovanni, and A. Toschi, Non-perturbative intertwining between spin and charge correlations: A "smoking gun" single-boson-exchange result, SciPost Phys. **16**, 054 (2024).

[78] T. Schäfer, G. Rohringer, O. Gunnarsson, S. Ciuchi, G. Sangiovanni, and A. Toschi, Divergent precursors of the Mott-Hubbard transition at the two-particle level, Phys. Rev. Lett. **110**, 246405 (2013).

[79] V. Janiš and V. Pokorný, Critical metal-insulator transition and divergence in a two-particle irreducible vertex in disordered and interacting electron systems, Phys. Rev. B **90**, 045143 (2014).

[80] E. Kozik, M. Ferrero, and A. Georges, Nonexistence of the Luttinger-Ward functional and misleading convergence of skeleton diagrammatic series for Hubbard-like models, Phys. Rev. Lett. **114**, 156402 (2015).

[81] A. Stan, P. Romaniello, S. Rigamonti, L. Reining, and J. A. Berger, Unphysical and physical solutions in many-body theories: from weak to strong correlation, New J. Phys. **17**, 093045 (2015).

[82] R. Rossi and F. Werner, Skeleton series and multivaluedness of the self-energy functional in zero space-time dimensions, J. Phys. A: Math. Theor. **48**, 485202 (2015).

[83] T. Ribic, G. Rohringer, and K. Held, Nonlocal correlations and spectral properties of the Falicov-Kimball model, Phys. Rev. B **93**, 195105 (2016).

[84] R. Rossi, F. Werner, N. Prokof'ev, and B. Svistunov, Shifted-action expansion and applicability of dressed diagrammatic schemes, Phys. Rev. B **93**, 161102(R) (2016).

[85] O. Gunnarsson, T. Schäfer, J. P. F. LeBlanc, J. Merino, G. Sangiovanni, G. Rohringer, and A. Toschi, Parquet decomposition calculations of the electronic self-energy, Phys. Rev. B **93**, 245102 (2016).

[86] T. Schäfer, S. Ciuchi, M. Wallerberger, P. Thunström, O. Gunnarsson, G. Sangiovanni, G. Rohringer, and A. Toschi, Nonperturbative landscape of the Mott-Hubbard transition: Multiple divergence lines around the critical endpoint, Phys. Rev. B **94**, 235108 (2016).

[87] O. Gunnarsson, G. Rohringer, T. Schäfer, G. Sangiovanni, and A. Toschi, Breakdown of traditional many-body theories for correlated electrons, Phys. Rev. Lett. **119**, 056402 (2017).

[88] W. Tarantino, B. S. Mendoza, P. Romaniello, J. A. Berger, and L. Reining, Many-body perturbation theory and non-perturbative approaches: screened interaction as the key ingredient, J. Phys.: Condens. Matter **30**, 135602 (2018).

[89] J. Vučičević, N. Wentzell, M. Ferrero, and O. Parcollet, Practical consequences of the Luttinger-Ward functional multivaluedness for cluster DMFT methods, Phys. Rev. B **97**, 125141 (2018).

[90] P. Chalupa, P. Gunacker, T. Schäfer, K. Held, and A. Toschi, Divergences of the irreducible vertex functions in correlated metallic systems: Insights from the Anderson impurity model, Phys. Rev. B **97**, 245136 (2018).

[91] C. Melnick and G. Kotliar, Fermi-liquid theory and divergences of the two-particle irreducible vertex in the periodic Anderson lattice, Phys. Rev. B **101**, 165105 (2020).

[92] A. J. Kim and V. Sacksteder, Multivaluedness of the Luttinger-Ward functional in the fermionic and bosonic system with replicas, Phys. Rev. B **101**, 115146 (2020).

[93] E. G. C. P. van Loon, F. Krien, and A. A. Katanin, Bethe-Salpeter equation at the critical end point of the Mott transition, Phys. Rev. Lett. **125**, 136402 (2020).

[94] K. Van Houcke, E. Kozik, R. Rossi, Y. Deng, and F. Werner, Physical and unphysical regimes of self-consistent many-body perturbation theory, arXiv:2102.04508 [cond-mat.str-el].

[95] E. A. Stepanov, S. Brener, V. Harkov, M. I. Katsnelson, and A. I. Lichtenstein, Spin dynamics of itinerant electrons: Local magnetic moment formation and berry phase, Phys. Rev. B **105**, 155151 (2022).

[96] E. G. C. P. van Loon, Two-particle correlations and the metal-insulator transition: Iterated perturbation theory revisited, Phys. Rev. B **105**, 245104 (2022).

[97] A. J. Kim and E. Kozik, Misleading convergence of the skeleton diagrammatic technique: when the correct solution can be found, arXiv:2212.14768 [cond-mat.str-el].

[98] M. Pelz, S. Adler, M. Reitner, and A. Toschi, Highly non-perturbative nature of the Mott metal-insulator transition: Two-particle vertex divergences in the coexistence region, Phys. Rev. B **108**, 155101 (2023).

[99] L. Del Re and G. Rohringer, Fluctuations analysis of spin susceptibility: Néel ordering revisited in dynamical mean field theory, Phys. Rev. B **104**, 235128 (2021).

[100] In contrast, for the situation of the generalized susceptibility in the *pp* channel, see the Supplemental Material [67].